Hindawi
Advances in Civil Engineering
Volume 2018, Article ID 2940169, 12 pages
https://doi.org/10.1155/2018/2940169

Research Article

Comparative Study on the Performance of Blended and Nonblended Fly Ash Geopolymer Composites as Durable Construction Materials

Debabrata Dutta and Somnath Ghosh

Department of Civil Engineering, Jadavpur University, 188 Raja S.C. Mallick Road, Kolkata 700032, India

Correspondence should be addressed to Debabrata Dutta; ddebabrata83@gmail.com

Received 20 August 2017; Accepted 27 December 2017; Published 19 February 2018

Academic Editor: Robert Černý

This article represents that the mechanical and microstructural properties and durability of fly ash-based geopolymers blended with silica fume and borax are better than those of conventional fly ash-based geopolymers. Fly ash itself contains the sources of silica and alumina which are required for geopolymerisation. But a sufficient amount of high-reactive silica is able to rapidly initiate geopolymerisation with activation. Pure potassium hydroxide pellets and sodium silicate solution were used for preparation of alkaline activator solution. Fly ash geopolymer paste exhibited better mechanical properties in the presence of silica fume with slight portion of borax. The effect of silica fume-blended geopolymer paste on temperature fluctuation (heating and cooling cycle at certain temperatures) showed better performance than nonblended fly ash-based specimens. Durability property was evaluated by immersion of geopolymer specimens in 10% magnesium sulfate solution for a period of one year. The change in weight, strength, and microstructure was studied and compared. In the magnesium sulfate solution, a significant drop of strength to around 37.26% occurred after one year for nonblended fly ash-based specimens. It is evident that specimens prepared incorporating silica fume had the best performance in terms of their properties.

1. Introduction

Numerous studies have already been done on fly ash-based geopolymers, as fly ash contains large amounts of silica and alumina. It is also clear that the reaction process basically involves alkaline activation of the source material by alkali hydroxide and sodium silicate solution followed by heat curing [1]. Again, this material exhibits good strength and durability when compared to conventional concrete [2]. The geopolymer chemistry elaborates the formation of 3D polymeric chain by Si–O–Al–O bond during the reaction between the source material rich in silica and alumina [3]. But the chemistry of geopolymers is altered for different combinations of raw material and alkalis [4]. The higher viscosity of the activator interferes with the rheological characteristics of the geopolymers. Thus, the porosity of geopolymers increases for finer precursor materials [5]. Inclination is needed towards several disposals over fly ash as the supplemental material in geopolymers like silica fume. Silica fume is a very fine material (particle size ranging from 1 μm to 15 μm). The basic problem in using silica fume as a base material for geopolymers is the absence of aluminium (trivalent in character). This phenomenon may be overcome with two different alternatives. The primary one is the choice of an activator, and the second one is the intrusion of secondary material. The choice of an activator is subjected to specific chemistry. Higher presence of monomers and dimers which exists during dissolution of Al–Si appreciates sodium hydroxide for better stabilization. Again, for larger silicate oligomers, potassium hydroxide is preferred for better coordination [6]. Latest research exhibits typical geopolymer varieties from simple to multiple phases. In the present research, silica fume was incorporated in fly ash-based geopolymers. Commercial borax (like substitute of aluminium) was used as another secondary input in the mixture. Borax arises in nature as evaporated dump formed by the continual evaporation of seasonal lakes. The effectiveness of

the pioneer composite was studied by comparing typical parameters like strength and durability with traditional fly ash-based geopolymers.

2. Chemistry of the Study

Fly ash activated with sodium hydroxide sometimes creates cracks with aging [7]. It is because of continuous pore pressure developed within the hardened composite by the late precipitated alkali compound [7]. However, at the initial level, it shows successive strength gaining for the time being [7]. On the contrary, potassium hydroxide is better for developing stable structures only under higher concentration of sodium silicate [8]. Earlier studies depict that despite having the same electric charges, the Na^+ and K^+ act in a different way because of dissimilar size. The smaller cation favors the ion-pair reaction with the smaller silicate oligomers, like silicate monomers, dimers, and trimers [9–11]. Xu et al. observed that the smaller silicate oligomers like monomers and dimer are better stabilized by Na^+ (sodium ion) and result in higher extent of dissolution, whereas more silicate solution emphasizes larger silicate oligomers which can be better coordinated by K^+ cation of larger size [6]. The previous study showed stable compressive strength for fly ash-based geopolymers activated with potassium hydroxide with higher concentration of sodium silicate [12]. The major drawback of this geopolymer composite is the rise in water content in the mixture. The higher amount of sodium silicate in fact allows the presence of additional water embedded within it. Consecutively, additional water makes the structure more porous, lesser in weight, and mainly permeable to some extent. Based on the discussed theory, a suitable compensator of sodium silicate has been evaluated in this study where silica fume has been introduced as the primary source of reactive silica to initiate the faster reaction. The presence of a higher oligomer in the chemical environment is favorable for the purpose of using potassium as the charge compensator or system stabilizer. Geopolymer is a Si–O–Al–O tetrahedral frame structure. But rise in the ratio of Si to Al may insist the formation of a chain-like structure over frame structure. So, another secondary input borax (B) has been typically applied in a manner to maintain the Si/X ratio, where X = Al or B, considering that both have three valence electrons. Another cause of choosing borax in this study is specifically to enhance the X content without allowing further incorporation of additional silica.

3. Experimental Procedure

3.1. Materials. The materials used in this research were class F fly ash (ASTM C618) produced by Kolaghat Thermal Power Plant, India; silica fume supplied by Oriental Trexim Pvt. Ltd., India; and commercial borax collected from DRD Educational & Consultancy Pvt. Ltd., India. In fly ash, 78% of the particles were finer than 45 microns with Blaine's specific surface area equal to 380 m^2/kg. The BET surface area of silica fume was 18,900 m^2/kg. Commercial borax had specific gravity and BET surface area equal to 1.7 and 557 m^2/kg, respectively. Potassium hydroxide pellets and sodium silicate solution were collected from Loba Chemie Limited, India.

3.2. Specimen Preparation. Alkaline activator was prepared by dissolving potassium hydroxide pellets directly into water. The dissolved hydroxide pellets were left at room temperature for 24 hrs. After that, predetermined quantity of sodium silicate solution was added 3 hours before being used for mixing as done earlier [13]. In the activator solution, the K_2O content was maintained at 6% of the total base material plus supplementary material (fly ash, silica fume, and borax). Apparent silicate modulus (SiO_2/K_2O) was kept as 1 and 0.1. Originally, silicate modulus in the activator has to be calculated from the formulation ($SiO_2/(K_2O + Na_2O)$). In this case, apparent silicate modulus is taken earlier for easier calculation. It is already described that Na^+ is essentially required to promote monomers, dimers, and trimers in the starting of activation. Here, a slight amount of sodium silicate solution was added in some cases only to confirm the presence of Na^+ in the mixture. The mixture was prepared in the model P660 Hobart mixer of capacity 600 cc and speed 60 cps. Fly ash with activator solution was mixed for 5 minutes. For blended mixtures, fly ash with supplementary material was mixed with activator solution for 5 minutes. The mixture was then transferred into a cubical mould and subjected to a table vibration for 2 minutes to expel entrapped air. After 60 minutes of rest period in open air, the cubes were cured in a hot air oven for a period of 48 hours at 85°C and allowed to cool inside the oven after that. The scanning electron micrographs and chemical composition of fly ash, silica fume, and borax are represented in Figure 1 and Table 1, respectively. The mix proportions of six sample mixes are elaborated in Table 2.

3.3. Test Details

3.3.1. Strength Test. Compressive strength of the specimens was tested by digital compression testing machine of model number EM500 supplied by Enkay Enterprise. The least count was 0.001 kN. The compressive strength of cube specimens was done as per ASTM C109.

3.3.2. Exposure Test in Sulfate Solution. Experimental setup was prepared to investigate the performance of blended and non-blended fly ash-based geopolymer samples in 10% concentration of magnesium sulfate solutions for one year. The test specimens (cubical) were immersed vertically in a glass pan. After immersion, the water level was maintained at 4 cm-5 cm over specimens. Throughout the exposure, regular investigations on physical appearance, residual strength, and weight changes were monitored at preselected intervals.

3.3.3. Physical Changes and Optical Microscopy. At preset intervals, the exposed geopolymer specimens were removed from the solutions and observed for any remarkable changes in its physical appearance. A crack detection microscope WF 10x, manufactured by C&D (Micro services) Ltd. (U.K.) was

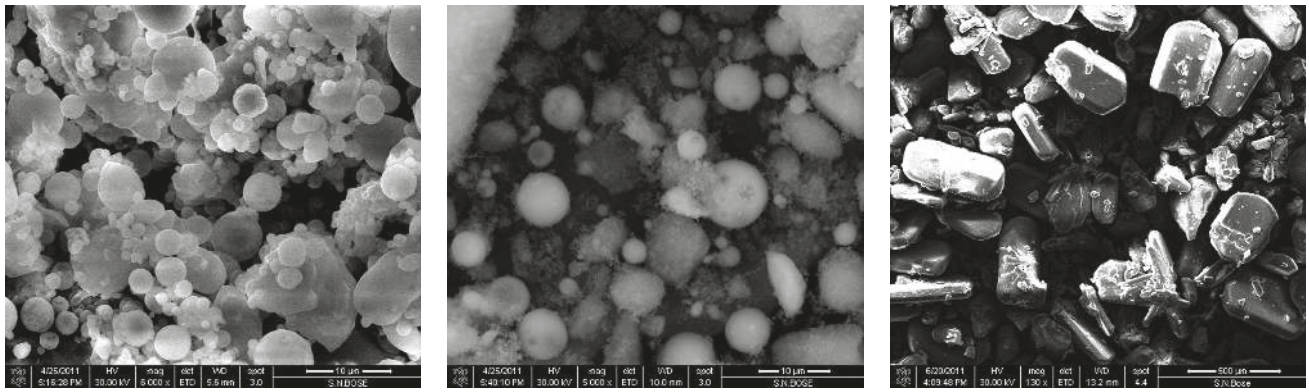

(a) (b) (c)

Figure 1: Scanning electron microscopic images of (a) fly ash, (b) silica fume, and (c) borax.

Table 1: Chemical composition of different raw materials (quantity in %).

Chemical composition	SiO_2	Al_2O_3	Fe_2O_3	TiO_2	CaO	MgO	K_2O	Na_2O	SO_3	P_2O_5	B_2O_3	LOI (%)
Fly ash	56.01	29.8	3.58	1.75	2.36	0.30	0.73	0.61	Nil	0.44	Nil	0.44
Silica fume	92.00	0.46	1.60	Nil	0.29	0.28	0.61	0.51	0.19	Nil	Nil	1.00
Borax	Nil	Nil	1.0	Nil	Nil	Nil	Nil	17.0	1.0	Nil	59.00	22.08

Table 2: Mix proportions of geopolymer mixes.

Sample ID	Fly ash* (%)	Silica fume* (%)	Borax* (%)	K_2O content in activator (%)	SiO_2 content in activator (%)	Water* (%)
SMF1	100	0	0	6	6	33
SMF2	100	0	0	6	0.6	33
SMS1	90	10	0	6	6	33
SMSB1	90	7.5	2.5	6	6	33
SMSB2	90	5.0	5.0	6	6	33
SMSB3	90	5.0	5.0	6	0.6	33

*This is the percentage amount with respect to the total weight of fly ash, silica fume, and borax. Calculated as the % of (fly ash + silica fume + borax); measured by weight.

used to detect the surface changes of the specimens at preset intervals throughout the exposure period. Observations on unexposed samples were conducted for making comparison with exposed samples.

3.3.4. Change in Weight. Before immersion in saline water, every specimen was kept submerged in potable water for 1 hour. After that, the samples were taken out and weighed. This measured weight value was indicated as the primary weight for individual. Specimens were weighed after every preselected interval. Before weighing, the specimens were clothed and brushed out to remove the free water and needle-like outcome (if any). Here, simple scrub brushes and cotton cloth were used for cleaning. Every specimen was brought to a saturated surface dry condition by applying mild airflow over the specimens for 5 minutes. Digital electronic balance of least count equal to 0.001 gm was used to conduct weighing. Change in weight indicates the percentage change (increment or decrement) with respect to the primary data at different intervals.

3.3.5. Change in Strength and Residual Strength. The average strength of any defined series of sample before the first immersion in the setup was treated as the primary strength value for specimens. A set of ten samples of different series were subjected to strength test at preselected intervals. Before testing, the specimens were kept at room temperature under airflow for 24 hrs. Digital electronic balance of least count equal to 0.001 gm was used to conduct weighing. The percentage change in strength (+/−) with respect to the primary strength value at different intervals is evaluated. The residual strength indicates the percentage of strength achieved at different intervals to the primary strength value. The residual strength at any interval is expressed as "100 − percentage change in strength."

3.3.6. Thermal Fluctuation Setup. A chest freezer of Model No. VT3-NUCAB 400L with glass-top configuration supplied by Hindustan Unilever, India, has been used in this study. The temperature fluctuating domain is limited from 8°C to −20°C. Each specimen was subjected to 20 consecutive

Figure 2: Physical appearance of the samples: (a, b) SMS1, (c, d) SMSB1, and (e, f) SMSB2.

cycles for a program of almost 85 hours. At the initial phase, the specimens were allowed to cool at 8°C for 2 hours. After that, it was brought to −20°C for the immediate next 2 hours. The temperature change rate was reported almost as 2°C/minute.

3.3.7. Scanning Electron Microscopy. Scanning electron microscopy was conducted by QUANTA 2000 with a capacity of 2.4 nm at 30 kV at high vacuum condition. The geopolymer sample was collected as a small scrap form to conduct this study. Samples with irregular shape were collected at the time of crushing. For the research, scraps were collected from the inner part of the specimen under consideration. No further grinding or polishing was done for SEM analysis.

3.3.8. Mercury Intrusion Porosimetry. MIP samples were made by cutting a cylinder of ¼ in. diameter to ½ in. height, having a bulk sample volume of 1.00 cc, which were tested on Micromeritics Autopore II (Central Glass and Ceramic, India) from 0 to 60,000 psi, with Hg surface tension 480.00 erg/cm^2 and contact angles (I) 140.00° and (E) 140.00°. MIP was used to examine a statistical comparison of the tested samples in terms of mean and median pore size, pore distribution, total porosity, bulk density, and apparent density. The bulk volume of each test specimen was 1 cc, and the maximum applied intrusion pressure during the test was about 53,500 psi. In this method, mercury is intruded under pressure in an evacuated sample, and volume of intruded mercury is monitored against pressure. In the feature of this very test, the pore volume distribution over pore diameter is presented as a distribution function $F = -dV/d \log D$, where V is the collective pore volume and D the diameter of pores. It indicates that the part under

Table 3: Compressive strength at 3 days after heat curing.

Number	Sample ID	Compressive strength (MPa) at 3 days after heat curing
1	SMF1	14.25
2	SMF2	0.0
3	SMS1	—
4	SMSB1	18.62
5	SMSB2	29.05
6	SMSB3	28

a function of any pore diameter range capitulates pore volume of pores in that range.

3.3.9. Energy Dispersive X-Ray Analysis. Energy dispersive X-ray analysis was carried on a point of selected samples for SEM under QUANTA FEG 250. The geopolymer sample was collected as a small scrap form to conduct this study.

4. Results and Discussion

4.1. Physical Appearance. Excessive volumetric increment was observed for sample SMS1 (Figure 2). As silica fume is very reactive, it emphasizes the formation of dihydrogen by oxidation of free silicon by water of alkaline medium during synthesis [14]. In alkali-activated fly ash-based geopolymers, the purpose of sodium silicate is to start the polymerization at the earlier stage [13]. But, for blended geopolymers, silica fume helps the formation of in situ inorganic foam itself at the initial stage [14]. The volumetric enlargement of SMS1 was due to the increment in dihydrogen production by water in the presence of reactive silica fume. Further, the addition of external borax can better stabilize the structure macroscopically. Borax can play the role of alumina in a similar manner to compensate the additional requirement of alumina due to the presence of much reactive silica from silica fume.

4.2. Compressive Strength. At hardened state, compressive strength is considered as the characteristic material value for the identification of the structural feature. Table 3 presents the mean compressive strength of the six samples measured in digital compressive strength testing equipment. In this study, the noticeable feature was visualized in absence of sodium silicate for fly ash-based geopolymer SMF2. Figure 3 shows the disintegrated part of partially reacted geopolymer SMF2. Sample SMSB1 had almost a shape of fungus mushroom, where a swelled top has risen upon the perfect cube base. The swelled portion was cut out by using an electrically operated low-speed concrete saw cutter to obtain a perfect cube. Excessive swelling was observed for sample SMS1. Extrication of any right cubical unit from the honeycombed, asymmetrical, and distorted outcome of sample SMS1 was not possible. Because of that, sample SMS1 was not supportive for the measurement of compressive strength in test setup.

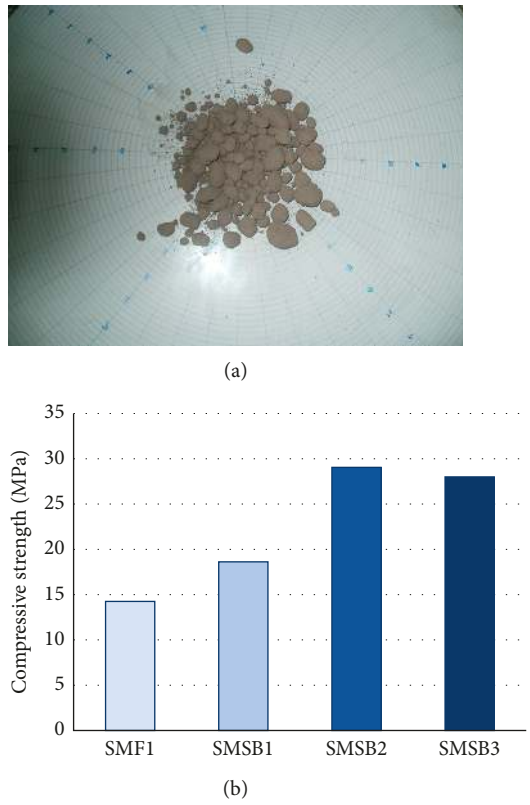

Figure 3: (a) Sample SMF2 after mixing and (b) compressive strength at the third day after curing.

Fly ash activation in the presence of external silica fume and borax sources yields a better geopolymer. Successive betterment in compressive strength was observed with the incorporation of silica fume and borax in certain percentage in the composition. Another important finding was that lowering of sodium silicate in mixing had little to no effect in polymerization or condensation process of silica fume-blended geopolymers (as treated for SMSB3). Maximum compressive strength was obtained for SMSB2 (29.05 MPa).

4.3. Thermal Fluctuation Effect. For a hardened geopolymer, it can be assumed that the most thermal sensitive part within the geopolymer composite is the crystalline alkali precipitation. In Figures 4(a) and 4(b), the regular crystal structure within the pore indicates the presence of alkali. Point A indicates alkaline surplus within the pores of the geopolymer body for fly ash-based geopolymers. In Figure 5, EDAX shows the existence of sodium-based alkaline precipitation, at point A. This entrapped crystal compound is basically due to the late and less reaction. In fact, alkali hydroxide is essential for the dissolution of silica and alumina. The metallic cations (Na, K, and others) maintain the structure neutrality as aluminium has fourfold coordination. But, alkali metal hydroxide which acts as a catalyst expelled out during the hardening of the gel phase with the progression of reaction [15]. In this research, it is supposed that incorporation of

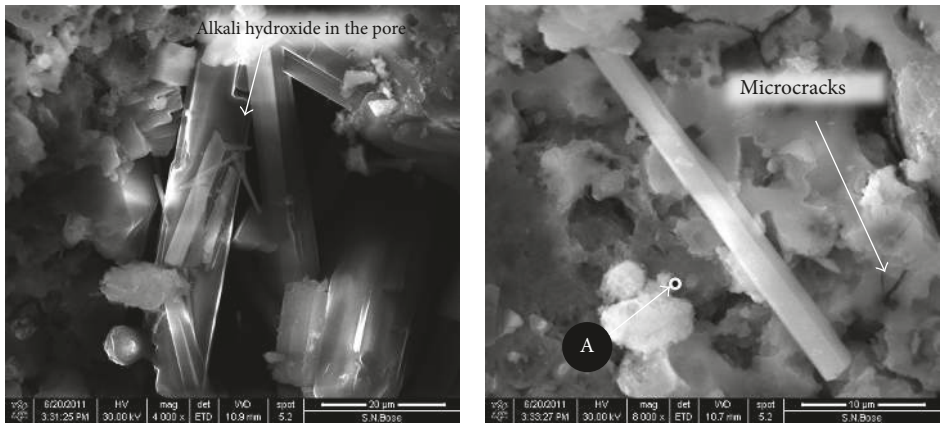

(a) (b)

Figure 4: (a) Crystal structure within SMF1. (b) After fatigue exposure, microcracks in SMF1.

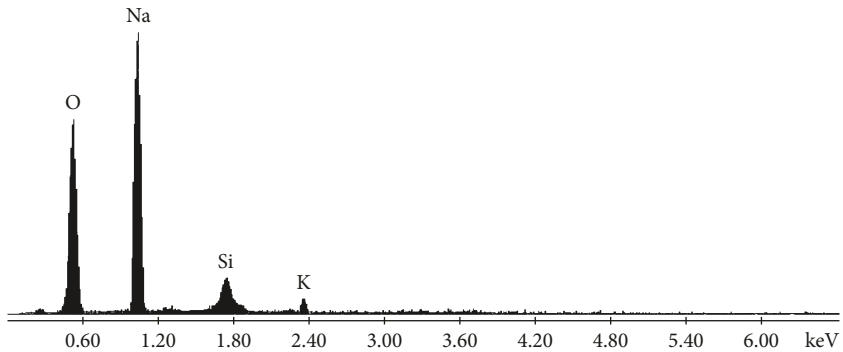

Figure 5: EDAX analysis at the position near A.

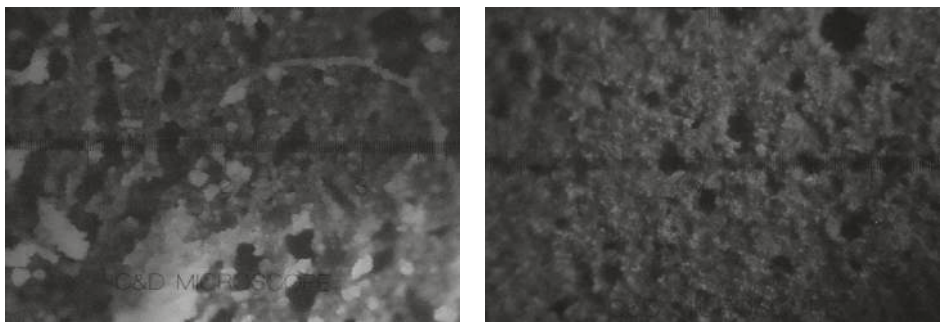

(a) (b)

Figure 6: Optical microscopy (10x magnification). Sample SMF1 (a) and sample SMSB2 (b) after 30 days.

silica fume emphasizes the speed of reaction which allows the expulsion of metal hydroxide instantaneously. The existence of the entrapped alkaline entity in the nonblended composites after hardening possibly resulted from the slower rate of reaction. Now, the temperature fluctuation affects the volumetric change of alkali solution within the pore. This can cause remarkable fatigue on the geopolymer skeleton and successive crack formation (as shown in Figure 4(b)). The result shows failure for sample SMF1 at the end of temperature fluctuating cycles.

4.4. Efflorescence Behavior (Study at Micro- and Macrolevel). Geopolymer efflorescence is the outcome from the geopolymer body which is highly alkaline. The charge compensator alkali hydroxide basically extrudes from the pores with the process of synthesis or the formation of Si–O–Al. Basically, alkali metal hydroxide acts as a catalyst, but almost the same amount which is added during synthesis is leached out from the hardened structure [15]. Moderate amount of late leaching was noticeable for sample SMF1 under optical microscopy (as shown in Figure 6(a)). But silica

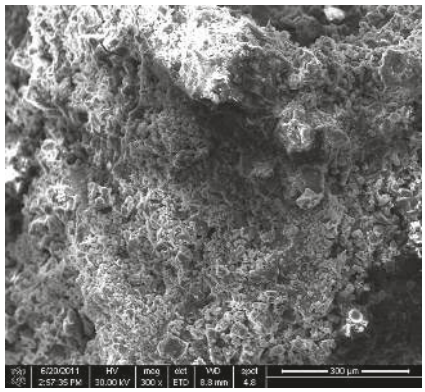

(a)

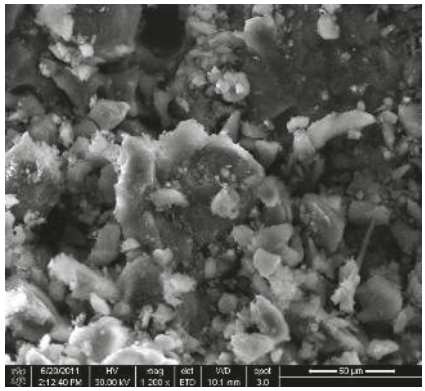

(b)

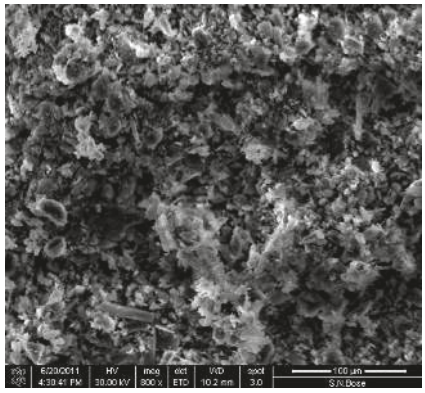

(c)

Figure 7: (a) Outer surfaces of sample SMF1 at 3 days (a), 30 days (b), and 60 days (c) from the end of heat curing.

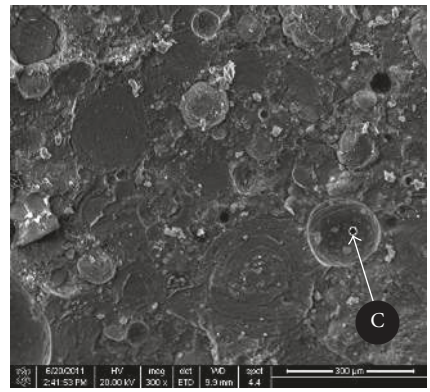

(a)

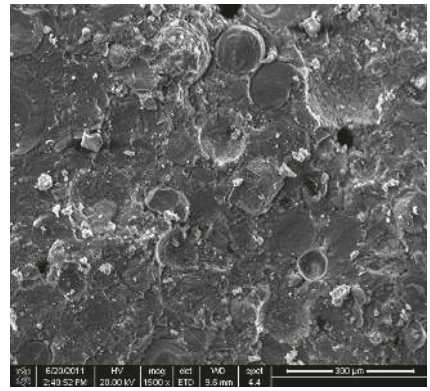

(b)

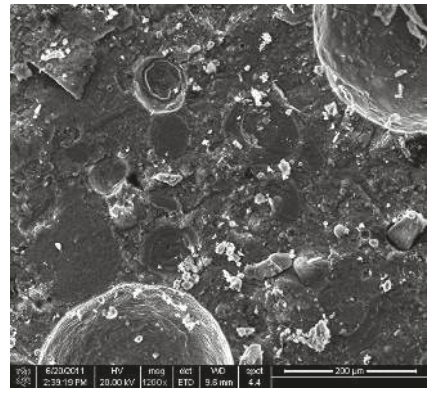

(c)

Figure 8: (a) Outer surfaces of sample SMSB2 at 3 days (a), 30 days (b), and 60 days (c) from the end of heat curing.

fume-blended geopolymers did not exhibit such characteristics (as shown in Figure 6(b)). It is because of the presence of silica fume which makes a very reactive complex and compact structure. Generally, the application of sodium silicate initializes the primary polymerization, but for the blended mix, this role is almost taken by the reactive silica fume [16]. Excessive leaching was observed under scanning electron microscopy for sample SMF1 with aging. Figures 7(a)–7(c) represent the SEM images of sample SMF1 at the age of 3, 30, and 60 days. The sample SMSB2 did not show excessive leaching with aging. Figures 8(a)–8(c) show compact and intact structure supporting strong alkali silicate reaction product as defined by point *C* in Figure 8(a).

4.5. Durability Study in Magnesium Sulfate Exposure. Samples SMF1, SMS1, SMSB1, SMSB2, and SMSB3 were immersed in 10% magnesium sulfate solution for 12 months. The methodology was the same as Thokchom et al. taken earlier [17]. At a preselected interval, the physical appearance of geopolymer specimens was examined. Elongated needle-like crystal formation began appearing on the surfaces of sample SMF1 after few weeks (as shown in Figure 9(a)).

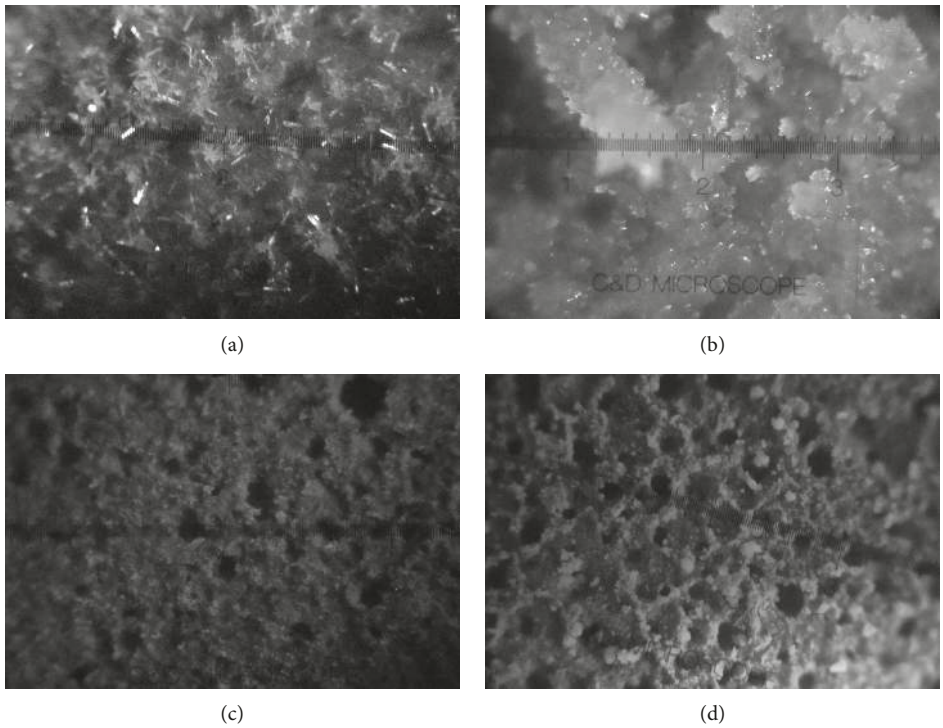

Figure 9: (a) Sample SMF1 showing a needle-like structure after 1 month of exposure to magnesium sulfate solution (optical microscope at 10x magnification). (b) Sample SMF1 showing white precipitant after 6 months of exposure to magnesium sulfate solution (optical microscope at 10x magnification). (c) Sample SMSB2 showing the fresh surface after 1 month of exposure to magnesium sulfate solution (optical microscope at 10x magnification). (d) Sample SMSB2 showing very little precipitants on the surface after 6 months of exposure to magnesium sulfate solution (optical microscope at 10x magnification).

These images of surfaces of the specimens were observed under an optical microscope with a magnification of 10x. After 12 weeks of exposure in 10% magnesium sulfate solution, sample SMF1 showed needle-like elongated crystal formation. It is due to the reaction of alkali hydroxide (within the pores) with magnesium sulfate, which forms less-soluble magnesium hydroxide with precipitation of alkali sulfate. White precipitant in larger quantity was observed for sample SMF1 after 6 months (as shown in Figure 9(b)), which may be magnesium hydroxide with sodium sulfate. Again, it was confirmed through scanning electron microscopy (as shown in Figures 10(a) and 10(b)) and EDAX analysis (as shown in Figure 10(c)) of scrap taken from the inner part of the sample. This outcome was the basic cause behind the drop in weight and strength after 9 months for sample SMF1. Bakharev [18] reported that the loss of strength is due to the migration of alkalis from the specimens and also due to the diffusion of calcium and sulfur near the surface region. But samples SMSB2 and SMSB3 did not show any formation at the outer surface for the time being during sulfate exposure (as shown in Figures 9(c) and 9(d)).

4.6. Change in Weight and Residual Strength. The result shows a remarkable increment in the weight of the non-blended samples exposed to magnesium sulfate solution at room temperature up to 3 months (Figure 11(a)). The similar trend was observed for compressive strength (Figure 11(b)). But materials blended with silica fume and borax did not show any remarkable change in connection with weight and strength. As mentioned earlier, the entrapped alkali within the pores of geopolymers participates in the ionic transaction in the presence of magnesium sulfate. This phenomenon has a great impact on the change in weight and strength for the time being during sulfate exposure. Again, the volumetric change within the pores enhances the pore pressure. This may be treated as the initial cause of strength increment. But later on, this continuous change in volume (compound within the pore) deteriorates the polymer structure. Due to the lack of the presence of the untreated hydroxide within the pore, silica fume-based geopolymers did not exhibit in this manner. The drop in compressive strength of sample SMF1 was around 37.26%. But there was almost no such change for SMSB2. The detail of change in weight and strength at different times of exposure to sulfate solution (as a percentage of primary value) is plotted in Figures 11(a) and 11(b), respectively. The figures indicate a noticeable drop from the primary values in connection with weight and strength for the SMF1 specimen.

The results of volume intrusion of the MIP of geopolymers are shown in Figure 12. The volume intrusion down to 1 micrometer was indicated for sample SMSB2. The results of volume intrusion of samples clearly reflect the change in chemistry with the change in the constituent materials. The

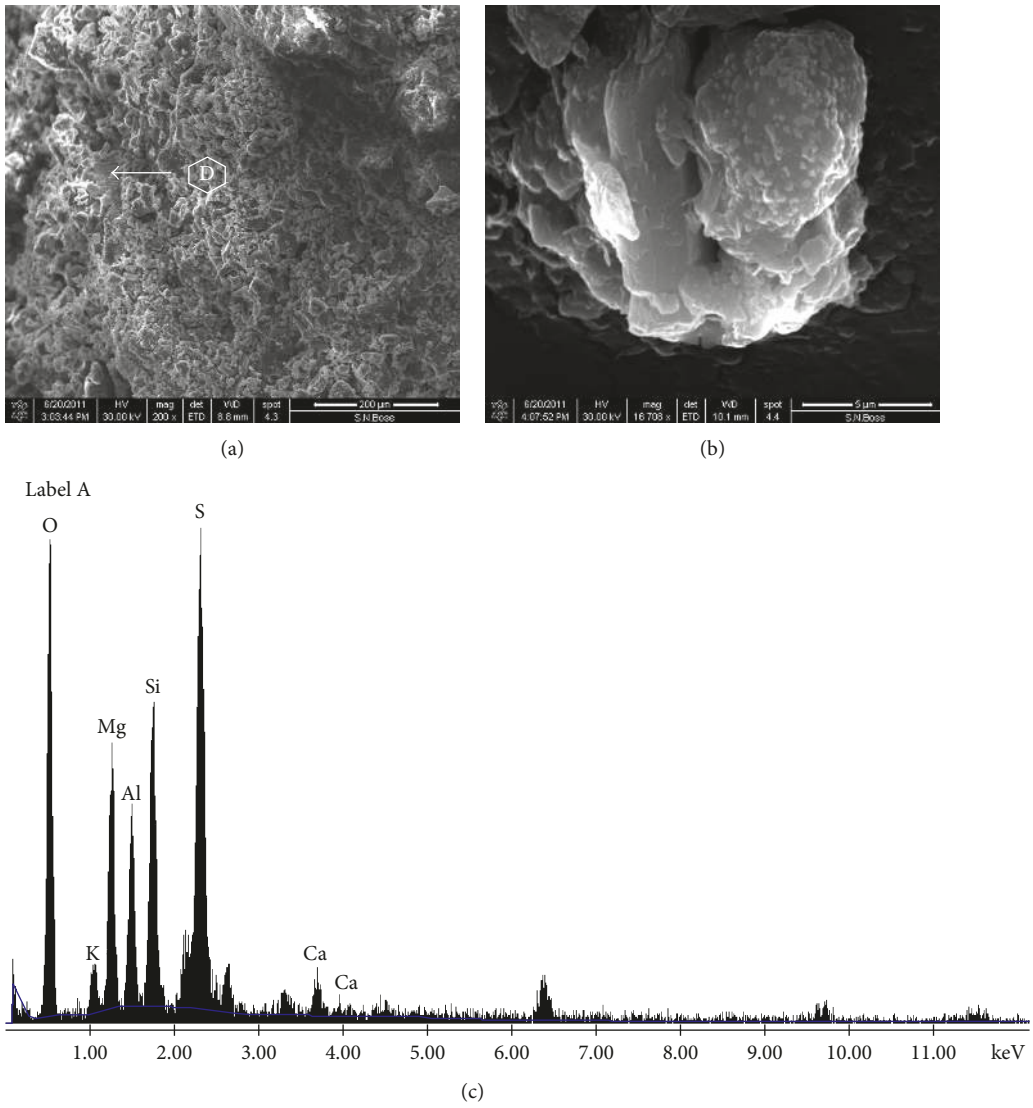

Figure 10: (a) Sample SMF1 showing white precipitant at the inner surface after 3 months at 200x magnifications. (b) SEM analysis near point D at 16708x magnification. (c) EDAX analysis at point D.

fine silica fume with high surface area eased the dissolution of silica which resulted in higher rate of reaction and produced denser matrix with higher compressive strength. Reactive silica fume significantly produced higher percentage of larger pores with a lower limit greater than 10 micrometers (the specimens SMS1 and SMSB1). The study reveals that geopolymer is a tetrahedral aluminosilicate structure. This structure (Al–O–Si) consisting of aluminium and silica is interlinked tetrahedrally by allotting alternate oxygen atoms. But based on the Si/Al atomic ratio, the geopolymeric aluminosilicate structure diverges in different families from amorphous to semicrystalline frameworks like polysialate type (Si–O–Al–O–), polysialate-siloxo type (Si–O–Al–O–Si–O–), and polysialate-disiloxo type (Si–O–Al–O–Si–O–Si–O–) [19]. For samples SMS1 and SMSB1, the excessive rise in Si/Al ratio (due to the incorporation of reactive silica supplements) may insist the possible formation of Si–O–Si chain structure rather than any framework structure. However, sample SMSB2 again tends to form framework structure because of the presence of borax containing boron (B). Here, the role of aluminium (Al) is compensated by boron (another fourfold). The difference in pore morphology must signify the change in structural formation.

Figure 12(d) illustrates the curve located within a small area for SMSB2. This indicates that the silica fume-blended geopolymers in the presence of borax reduces the mean pore size. Also, the threshold volume intruded values for the nonblended geopolymer SMF1 are larger than other silica-blended specimens. Thus, the reduced total volume of porosity and better pore size distribution contribute to the strength development.

5. Conclusions

Based on the experimental investigation, it is concluded that silica fume-blended fly ash-based geopolymers leads

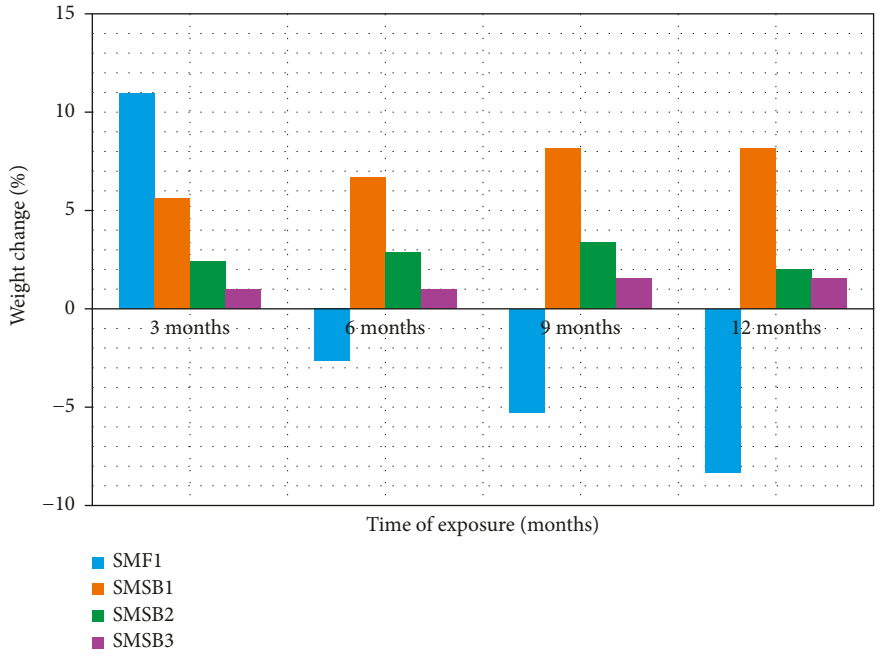

(a)

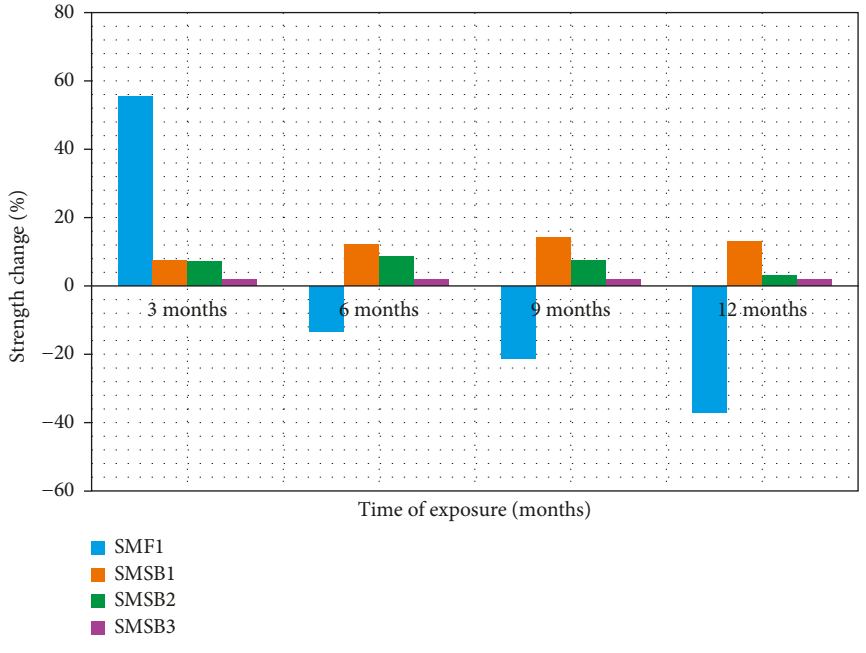

(b)

Figure 11: Percentage gain or loss in (a) weight and (b) strength with time of exposure to magnesium sulfate.

to a new trend which appears to generate more amorphous products and accelerates the rate of reaction in lower alkalinity. Sample SMSB3 (activated with very low value of sodium silicate) showed the compressive strength of 28 MPa after just 3 days, which is 96.49% greater than the compressive strength of sample SMF1. The maximum compressive strength (29.05 MPa) was obtained for SMSB2 (90% fly ash, 10% silica fume, and 5% borax-made specimens). Almost no efflorescence was observed for sample blended with silica fume in the presence of borax. Temperature fluctuation has little to no effect in microstructure and mechanical properties of silica fume and borax-blended geopolymers when compared to the geopolymer produced from only fly ash. The resistance to sulfate attack for silica fume and borax-blended geopolymers was excellent and almost stable in connection with weight and strength change. The threshold values of the intruded volume pore sizes and distribution confirm dense

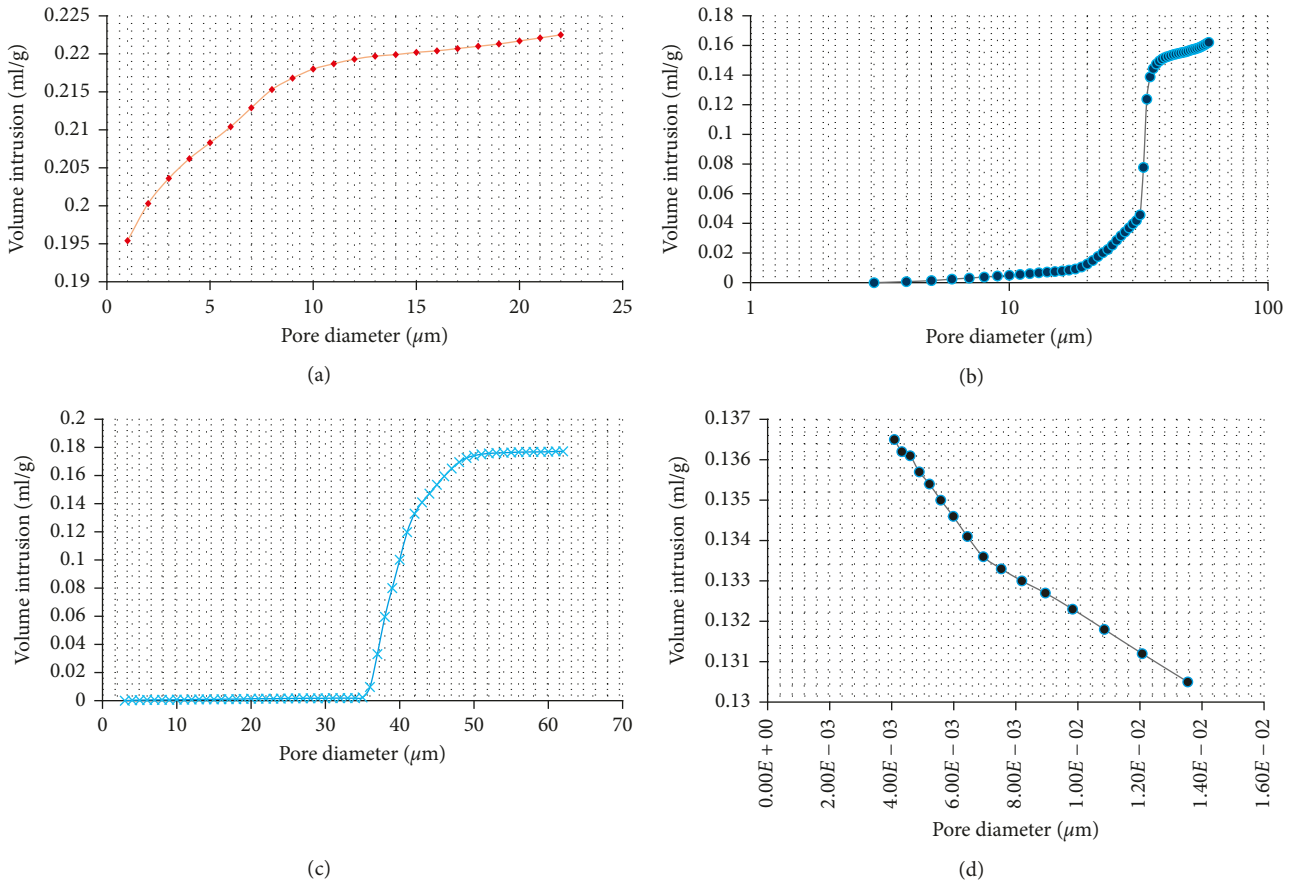

Figure 12: Intruded volume of MIP of geopolymers. (a) Sample SMF1, (b) sample SMS1, (c) sample SMSB1, and (d) sample SMSB2.

microstructure for silica fume and borax-incorporated fly ash-based geopolymers.

Conflicts of Interest

The authors declare that they have no conflicts of interest.

References

[1] J. G. S. van Jaarsveld, J. S. J. van Deventer, and G. C. Lukey, "The effect of composition and temperature on the properties of fly ash- and kaolinite-based geopolymers," *Chemical Engineering Journal*, vol. 89, no. 1–3, pp. 63–73, 2002.

[2] T. Bakharev, J. G. Sanjayan, and Y. B. Cheng, "Resistance of alkali-activated slag concrete to acid attack," *Cement and Concrete Research*, vol. 33, no. 10, pp. 1607–1611, 2003.

[3] E. I. Diaz, E. N. Allouche, and S. Eklund, "Factors affecting the suitability of fly ash as source material for geopolymers," *Fuel*, vol. 89, no. 5, pp. 992–996, 2010.

[4] E. P. Marinho, *Desenvolvimento de Pastas Geopoliméricas Para Cimentação de Postos de Petr´oleo*, Universidade Federal do Rio Grande do Norte, BrazilUniversidade Federal do Rio Grande do Norte, 2004 Ph.D. thesis, Thesis.

[5] P. H. R. Borges, L. F. Fonseca, V. A. Nunes, T. H. Panzera, and C. C. Martuscelli, "Andreasen particle packing method on the development of geopolymer concrete for civil engineering," *Journal of Materials in Civil Engineering*, vol. 26, no. 4, pp. 692–697, 2014.

[6] H. Xu and J. S. J. van Deventer, "The geopolymerisation of aluminosilicate minerals," *International Journal of Mineral Processing*, vol. 59, no. 3, pp. 247–266, 2000.

[7] D. Dutta and S. Ghosh, "Microstructure of fly ash geopolymer paste with blast furnace slag," *Current Advances in Civil Engineering*, vol. 2, no. 3, pp. 95–101, 2014.

[8] D. Dutta and S. Ghosh, "Parametric study of geopolymer paste with the different combination of activators," *International Journal of Engineering Innovation & Research*, vol. 3, no. 6, pp. 786–793, 2014.

[9] A. V. Mc Cormick, A. T. Bell, and C. J. Radke, "Evidence from alkali metal NMR spectroscopy for ion pairing in alkaline silicate solution," *Journal of Physical Chemistry*, vol. 93, no. 5, pp. 1733–1737, 1989.

[10] W. M. Hendricks, A. T. Bell, and C. J. Radke, "Effect of organic and alkali metal cations on the distribution of silicate anions in aqueous solutions," *Journal of Physical Chemistry*, vol. 95, no. 23, pp. 9513–9518, 1991.

[11] T. W. Swaddle, J. Salerno, and P. A. Tregloan, "Aqueous aluminates, silicates and aluminosilicates," *Chemical Society Reviews*, vol. 23, no. 5, pp. 319–325, 1994.

[12] D. Dutta, S. Chakrabarty, C. Bose, and S. Ghosh, "Comparative study of geo-polymer paste prepared from different activators," *STM Journals*, vol. 2, pp. 1–10, 2012.

[13] S. Thokchom, P. Ghosh, and S. Ghosh, "Durability of fly ash geopolymer mortars in nitric acid–effect of alkali (Na_2O) content," *Journal of Civil Engineering and Management*, vol. 17, no. 3, pp. 395–399, 2011.

[14] E. Prud'homme, P. Michaud, E. Joussein et al., "Silica fume as porogent agent in geo-materials at low temperature," *Journal of the European Ceramic Society*, vol. 30, no. 7, pp. 1641–1648, 2010.

[15] J. S. G. van Jaarsveld, J. S. J. van Deventer, and L. Lorenzen, "Factors affecting the immobilization of metals in geopolymerized fly ash," *Metallurgical and Materials Transactions, B*, vol. 29, no. 1, pp. 283–291, 1998.

[16] J. T. Gourley, "Geopolymers, opportunities for environmentally friendly construction materials," in *Proceedings of Conferenc in adaptive materials for a modern society*, vol. 49, 15–26, pp. 1455–1461, Institute of Materials Engineering Australia, Sydney, Australia, October 2003.

[17] S. Thokchom, D. Dutta, and S. Ghosh, "Effect of incorporating silica fume in fly ash geopolymers," *World Academy of Science, Engineering and Technology*, vol. 60, pp. 245–247, 2011.

[18] T. Bakharev, "Durability of geopolymer materials in sodium and magnesium sulfate solutions," *Paste and Concrete Research*, vol. 35, no. 6, pp. 1233–1246, 2005.

[19] J. Davitovits, "Geopolymers: inorganic polymeric new materials," *Journal of Thermal Analysis*, vol. 37, no. 8, pp. 1633–1656, 1991.